An Accelerated BEM Formulation for the Forward Problem Solution of ESI Using Realistic Head Models

Z. Akalın, N. G. Gençer
Department of Electrical and Electronics Engineering, Middle East Technical University, Ankara, Turkey

Abstract—**In this study, the forward problem of electrical source imaging (ESI) is solved using the Boundary Element method (BEM) with realistic head models. The realistic model consists of scalp, skull, CSF, brain and eyes. To get more accurate results quadratic elements are used in the meshes and a new method is proposed for the generation of the quadratic mesh. An accelerated method is proposed for the solution of the potential field.**

Keywords—**ESI, BEM, realistic head model, accelerated BEM, quadratic mesh.**

I. Introduction

The ultimate goal of this study is to solve the electric source imaging (ESI) problem more accurately and in a faster way. For this purpose, 1) realistic head models are generated 2) the BEM model is improved, and 3) simplifications are introduced on the forward problem solution.

In this work, a realistic model is developed that consists scalp, skull, CSF, brain and eyes. Triangular surface meshes are used for the conductivity boundaries. The BEM formulation allows the use of quadratic isoparametric elements [1]. To include the eyes into our model an automatic mesh generation algorithm is used for the intersecting surfaces [2] of the skull and eyes. A new approach is adopted to generate realistic head models with quadratic elements. For the computation of potentials the accelerated solution method introduced by Fletcher *et al* [3], is improved.

Next section explains the BEM formulation and the proposed method to increase the speed of the forward problem solutions. The results related to the use of recursive integration are presented. The third section introduces the approach used for the development of realistic head models.

II. Boundary Element Method

A. Formulation

The Boundary Element Method (BEM) is a numerical model for solving integral equations. It is employed in this study to calculate the electric potential due to an impressed current source in a conductive body. The related surface integrals are calculated numerically by dividing the surface into isoparametric elements. In the literature, different kinds of elements and methods are used to evaluate the surface integrals [4]. Using isoparametric elements in the formulations enables expressing both the global coordinates and potentials on an element using the same interpolation (shape) functions [1]. Linear, quadratic and cubic elements can be used. In this study, quadratic elements are used, which gives best results.

Integration over a surface element is written as a linear combination of unknown node potentials. If the potential is to be calculated at M nodes, then in matrix notation, it is possible to obtain the following matrix equation:

$$\begin{aligned} \mathbf{\Phi} &= g + \mathbf{C}\mathbf{\Phi} \\ \mathbf{A} &= \mathbf{I} - \mathbf{C} \\ \mathbf{\Phi} &= \mathbf{A}^{-1} g \end{aligned} \tag{1}$$

where $\mathbf{\Phi}$ is an $M\times1$ vector of node potentials, $\mathbf{C}$ is an $M\times M$ matrix whose elements are determined by the geometry and electrical conductivity of the layers, and g is an $M\times1$ vector representing the contribution of the primary sources. To eliminate the singularity in $\mathbf{C}$ matrix deflation is employed [5], and to overcome numerical errors caused by high conductivity difference around a layer, isolated problem approach (IPA) is implemented [6], [7]. $\mathbf{\Phi}$ can be solved using iterative methods such as the conjugate gradient method (CG) or directly by lower-upper (LU) decomposition. The details of the BEM formulation can be found in [1].

B. Accelerated BEM

Equation (1) provides the solution of the potential field at all nodes (in this study, it is around 10000). In the inverse problem solution, however, the potential field at the electrode positions $\mathbf{\Phi_e}$ is required. If m is the number of electrodes $\mathbf{\Phi_e}$ is a vector of $m\times1$ and can be expressed as follows:

$$\mathbf{\Phi}_e = \mathbf{D}\mathbf{A}^{-1} g \tag{2}$$

Here, $\mathbf{D}$ is a matrix composed of 0's and 1's and chooses the relevant rows of $\mathbf{A^{-1}}$. Thus if the selected rows of $\mathbf{A^{-1}}$ are calculated and stored, then $\mathbf{\Phi_e}$ can be calculated by a simple vector multiplication. In [3], a similar approach was recommended, however, the true inverse of $\mathbf{A}$ was calculated first and then its selected rows were multiplied by g to find the electrode potentials. Computing the true inverse of the $\mathbf{A}$ matrix is very expensive. In this study we

computed the required rows of $\mathbf{A}^{-1}$ by solving $\mathbf{A}^T x = e_i$ equation for each selected row.

Note that, any row of $\mathbf{A}^{-1}$ can be obtained by solving $\mathbf{A}^T x = e_i$ where e_i is a unit vector with 1 in the i^{th} entry (all the other entries are 0). With this method, all the m required rows of $\mathbf{A}^{-1}$ are computed using only m matrix solutions.

C. Recursive Integration

When the layers in Boundary Element mesh are close to each other, numerical errors occur. To prevent this the meshes can be made finer, but in this case the number of nodes increases and computation becomes costly. The accuracy of the BEM can be improved by the use of recursive integration [8] without refining the mesh. In recursive integration the surface elements are divided into smaller elements, over which the Gaussian integration is performed. The potential field is calculated at the original nodes, therefore no additional memory is required, but the number of integration points is increased, so the accuracy is improved. This process is repeated recursively with those sub elements until a subdivision criterion is met. For a mesh RDM (Relative Difference Measure) [5] is calculated with respect to iterations in integration.

A three layer spherical Rush and Driscoll [9] model is used, each layer having 512 elements and 1026 nodes. The radius of the shells are 9.2, 8.5, 8cm, and the conductivities are 0.2, 0.0025, 0.2S/m. It is observed that in the first iteration the RDM decreases from 28% to 1.5%. The average edge length for the outer layer is 1.1cm which is larger than the distance between the layers. In the first iteration, the effective element size becomes smaller than the distance between the layers and the RDM decreases. Further increasing the iterations RDM decreases slightly.

III. Development Of Realistic Head Models

A. Segmentation

In this work, segmentation is performed using the three-dimensional (3D) multimodal MR images of the head (T1, T2 and proton density (PD) images). A hybrid algorithm that uses snakes, region growing, morphological operations, and thresholding is applied to the images [10]. Scalp, skull, CSF, gray matter (GM), white matter (WM), eye tissues and eyeballs are segmented from the images. The details of the segmentation algorithm are given in [10]. The slice thickness in our images is 3mm and the resolution of the voxels of the MR images is 1×1×3mm. Therefore the segmented volumes have an apparent staircase effect, especially where there are rapid changes in the slices. In this study, the slices are interpolated and 2 additional slices are added between consecutive slices to improve the segmentation results.

B. Mesh Generation

In the mesh generation stage, first a very fine mesh is obtained by skeleton climbing. Next, the mesh is filtered and a coarsening process is performed according to Delaunay criteria. Thereafter, topological corrections are made. The details of the mesh generation algorithms can be found in [10] and [11]. In this study the generation of quadratic mesh generation is improved by inserting the algorithm in coarsening process. In the beginning of the coarsening, first linear elements are converted into quadratic elements. The coarsening is done by edge contraction due to an error criterion. When the edge of two elements would contract the middle nodes of the neighboring elements are moved to fit the original elements. Therefore the element groups of fine mesh are represented by quadratic elements in a lesser number.

While obtaining the whole mesh of the head, in some places where the CSF is very thin, the cortex and the skull touch each other (result of segmentation). While forming the mesh those regions may intersect or touch each other. Those regions are detected and the corresponding nodes are perturbed in their normal direction to prevent intersection.

To include the eyes into our model, an automatic mesh generation algorithm is used for intersecting surfaces. The eyes are situated in the cavities of the skull. The algorithm is applied to the outer surface of the skull and the eyes to obtain a unique mesh. The intersecting meshes are obtained using an algorithm based on [2].

The mesh generation algorithm for intersecting the skull and a single eye can be summarized as follows:

1. Find the intersections between skull and eye surfaces.
2. Determine a closed loop of intersection-line-segments.
3. Re-triangulate each intersecting triangle with new elements using the advancing front technique.
4. Identify resulting surface segments.
5. Remove the unnecessary elements.
6. Improve surface mesh quality.

The algorithm is repeated for the second eye.

IV. Results

In this study segmentation is applied to the axial MR images with 72 slices, 3 mm thickness. The resulting meshes of cortex, white matter, skull and scalp are presented in Fig.1. The intersecting surfaces of outer skull and eyes are presented in Fig. 2(a), the final mesh is presented in Fig. 2(b). The mesh consists of 9680 nodes, 4864 elements.

The computational complexity of the BEM solutions using a 933MHz Pentium III computer with 1.5 GB RAM is given in Table 1.

TABLE I
COMPUTATIONAL COMPLEXITY

Matrix filling	67 minutes
Single solution with CG	12 minutes
Calculation of the rows of the $\mathbf{A}^{-1}$ ($\mathbf{A}_e^{-1}$) matrix for 256 electrodes (256 solutions)	51.2 hours
Calculation of right hand side (RHS)	10 msec.
Calculation of $\mathbf{A}_e^{-1}$·RHS for 256 electrodes	0.12 sec

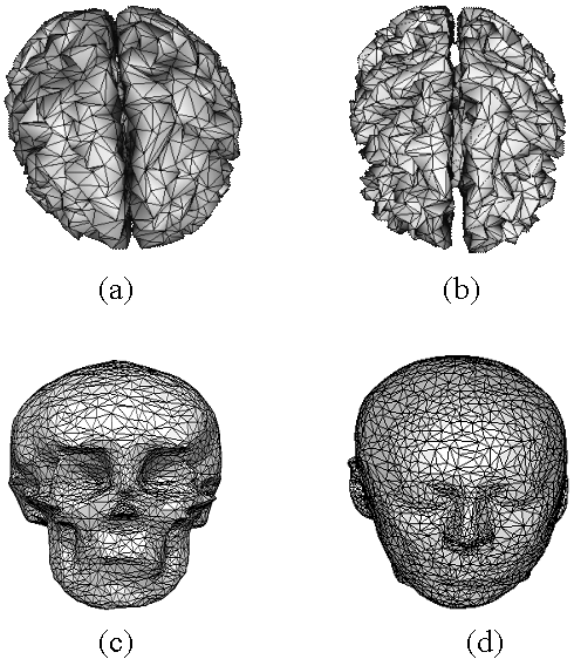

Fig. 1. Meshes of (a) cortex, (b) WM, (c) skull, (d) scalp.

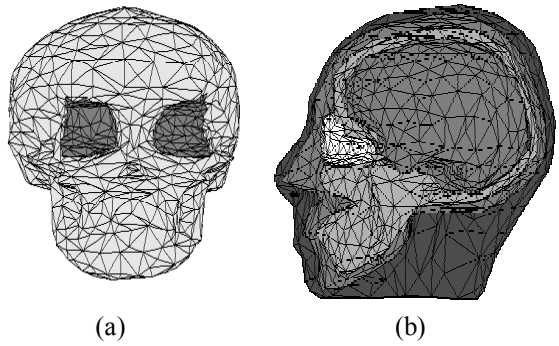

Fig. 2. (a) Intersecting mesh of the outer skull and the eyes. (b) Whole head mesh.

The segmentation algorithm takes 2 hours and the mesh generation algorithm takes 4 hours on the same computer. For solving the BEM matrix equation, the conjugate gradient method is used in this study.

V. CONCLUSION AND DISCUSSION

The BEM formulation used in this work was developed by [1]. The BEM program is updated to be able to use arbitrary meshes and intersecting surfaces. The accuracy of the original formulation is improved by using recursive integration. A fast method is suggested for the calculation of the scalp potentials.

A semi-automatic segmentation algorithm is developed to obtain a realistic head model representing the scalp, skull, cortex and eye tissues. This algorithm uses snakes algorithm, thresholding, morphological operations and region growing. It is observed that the segmentation algorithm is capable of detecting the main features of the tissues.

A hybrid mesh generation algorithm is developed to generate meshes for the segmented volumes. The mesh generation algorithm uses the skeleton climbing, filtering, coarsening and topological correction of the resulting meshes. The eye tissues are included into the model by the use of intersecting surfaces. A new method is suggested and implemented for the generation of the quadratic meshes.

An accelerated solution algorithm for computing forward problem solutions at the electrodes is introduced. Using this algorithm, solution time for a single dipole is reduced from 12 minutes to 0.12 seconds, once the selected rows of the matrix $\mathbf{A}^{-1}$ is computed. This work uses an unoptimized CG based solver for computing the rows of $\mathbf{A}^{-1}$. The preprocessing time can further be reduced by using different optimized iterative solvers. This approach is very useful for solving the inverse problem where the electrode potentials have to be computed for a very large number of dipoles.

ACKNOWLEDGMENT

The authors would like to thank Dr. Mehmet Çamurdanoğlu from Bayındır Hospital, Dr. Serdar Akyar from Ibni Sina Hospital and Dr. Suat Fitöz from Cebeci Hospital of Ankara for supplying and helping us analyzing the MR images.

This project is supported by METU research fund project AFP-2001-03-01-02.

REFERENCES

[1] N. G. Gençer, I. O. Tanzer, "Forward problem solution of electromagnetic source imaging using a new BEM formulation with high-order elements," *Phys. Med. Biol.*, vol. 44, pp. 2275-2287, 1999.

[2] A. A. Shostko, R. Lohner, W. C. Sandberg, "Surface Triangulation over Intersecting Geometries", *Int. J. for Numer. Methods in Eng.*, vol 44, pp. 1359-1376, 1999.

[3] D. J. Fletcher, A. Amir, D. L. Jewett, G. Fein, "Improved method for computation of potentials in a realistic head shape model", *IEEE Trans. On Biomed. Eng.*, vol. 42(11), pp. 1094-1104, 1995.

[4] S. Ueno, K. Iramina, K. Harada, "Effects of inhomogeneities in cerebral modeling for magneto-encephalography," *IEEE Trans. Magn.*, vol. 23, 3753-3755, 1987.

[5] M. S. Lynn, W. P. Timlake, "The use of multiple deflations in the numerical solution of singular systems of equations, with applications to potential theory", *SIAM Journal of Numerical Analysis*, vol. 5, pp. 303-322, 1968.

[6] J. Meijs, O. Weier, M. J. Peters, "On the Numerical Accuracy of the Boundary Element Method", *IEEE Trans. Biomed. Eng.*, vol. 36, pp. 1038-1049, 1989.

[7] M. S. Hamalainen and J. Sarvas, "Realistic Conductivity Geometry Model of the Human Head for Interpretation of Neuromagnetic Data", *IEEE Trans. on Biomedical Engineering*,, vol. 36(2), pp. 165-171, 1989.

[8] J. H. M. Frijns, S. L. de Snoo, R. Schoonhoven, "Improving the Accuracy of the Boundary Element Method by the Use of Second-Order Interpolation Functions", *IEEE Trans. On Biomed. Eng.*, vol. 47(10), pp. 1336-1346, 2000.

[9] S. Rush, D. A. Driscoll, "EEG Electrode Sensitivity -an application of reciprocity", *IEEE Trans. Biomed. Eng.*, vol. 16(1), pp. 15-22, 1969.

[10] Z. Akalın, C. E. Acar, N G. Gençer, "Development of Realistic Head Models for Electro-Magnetic Source Imaging of the Brain", *Proceedings of EMBC*, 2001.

[11] Z. Akalın, N. G. Gençer, "Investigating the effects of eye conductivity on EMSI forward problem using a realistic BEM head model", *Int. Journal of Bioelectromagnetism*, 219-220, 2002.